

Chapter 4. Results and Discussion

The results of applying the analytical approach described in “Guidelines for Detection, Analysis, and Treatment of Materials-Related Distress in Concrete Pavements – Volume 2 (Van Dam 2002b)” are summarized in this chapter of the report. Detailed test results for each bridge are provided in project portfolios in Appendix A.

4.1 Visual and Stereo Optical Microscope Analysis

The locations of each bridge evaluated and the observations of the cores made during the visual and stereo optical microscope examinations are summarized in table 1. In the observations provided in table 1, figures 1 through

4.2 Air-Void Analysis

The results of the air-void analysis by the modified point count method (ASTM C457) are summarized in table 2. Figure 8 plots the air contents and figure 9 the spacing factors for the cores evaluated. In order to evaluate the original air-void system of the samples, an attempt was made to record the number of filled air voids as well as the number of empty voids (ASTM C457, requires only the computation of the existing air voids, since only they can actually protect the paste against frost damage). Unfortunately, the BCPP staining method employed to selectively stain the ettringite filled voids purple did not provide the desired results, coloring both the paste and the filled voids light pink. This made it very difficult to observe a difference between the two. However, an approximate evaluation of the extent of the filled air voids had been recorded during the examination with the stereo optical microscope that preceded the staining procedure.

Table 1. Summary of core logs for sites included in this study.

| Core location/ Bridge ID | Year | WSU ID | MTU ID | Observations |
|--|------|-----------|-----------|--|
| I-75 over 13 Mi Rd S021-63174 | 2001 | 5 | A1 | 0.75-inch crushed tan carbonate coarse aggregate (limestone or dolomite). Gap in the gradation of the aggregates in A2 (figure 1). Small entrapped air voids, no rebar in the cores. Some fine cracked siltstones with aggregate-paste bond failure (cracks generally not extending far in the paste) (figure 2). |
| | | 8 | A2 | |
| I-75 over Clarkston Rd S15-63172 | 1989 | 6 | B1 | Mix of 0.75-inch crushed and natural gravel coarse aggregate. Rebar is present in both cores. A lot of irregularly shaped small entrapped air-voids around the aggregates and rebar (figure 3). No rust on the rebar. |
| | | 10 | B2 | |
| I-75 over Clintonville S12-63172 | 1988 | 6 | C1 | 0.75-inch natural gravel coarse aggregate. Rebar present in C2, no rust, well adhering paste. Some entrapped air voids (figure 3). |
| | | 10 | C2 | |
| I-75 over Auburn Rd S021-632174 | 2001 | 3 | D1 | 0.75 inch crushed tan carbonate coarse aggregate. Bad consolidation around the rebar in D1, no rust. Smaller gaps around some of the aggregates (figure 4). |
| | | 4 | D2 | |
| I-96 over M43 S02-23152A | 1980 | 1 | E1 | 0.75-inch natural gravel coarse aggregate. Rust on the rebar in both samples, paste does not adhere very well to it. Separation of the layer of concrete right above the corroded rebar in E2 (figure 5). |
| | | 5 | E2 | |
| I-94 over Merriman S04-82022 | 1993 | 6 | F1 | 0.75-inch blast furnace slag coarse aggregate. Big entrapped air void on one side of the rebar in F2, no rust. Some small entrapped air voids in the paste (figure 6). A lot of cracked fine cherts with reaction rims and cracked fine black siltstones, cracks go through the paste (a sign of ASR). Map cracking on the top surface of the cores. |
| | | 8 | F2 | |
| I-69 over Clark Rd S01-44044 | 1983 | 7 | G1 | 0.75-inch crushed tan carbonate coarse aggregate. Very poor consolidation (especially G2), a lot of entrapped air. Core G2 is broken in two pieces (figure 7). No rebar. |
| | | 10 | G2 | |
| I-94 over Middlebelt S06-82022 | 1993 | 2 | H1 | 0.75-inch blast furnace slag coarse aggregate. Some entrapped air-voids (figure 6). Rebar with a little rust on the sides is present only in H1. Several fine black siltstones with lengthwise crack, and cracked cherts with reaction rims, cracks go through the paste (a sign of ASR). |
| | | 4 | H2 | |

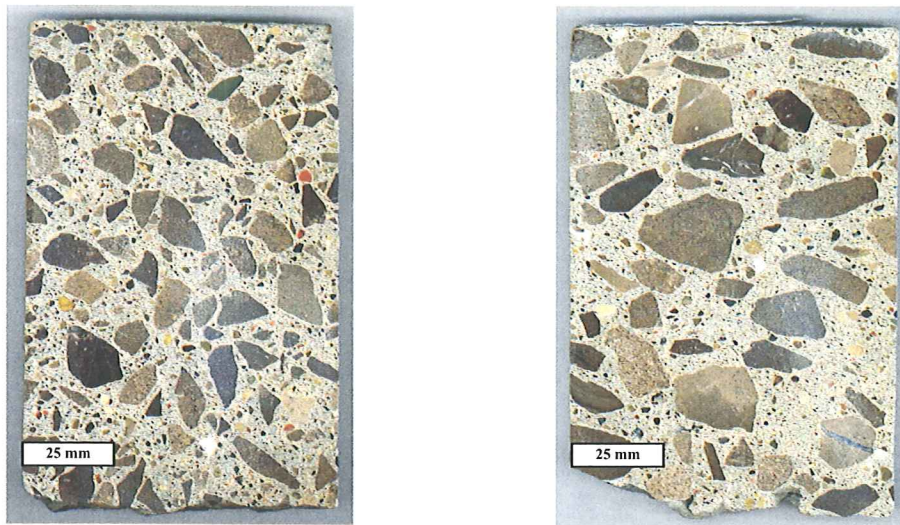


Figure 1. Difference in the gradation of the aggregates from core A1 (left) and A2 (right), polished slabs.

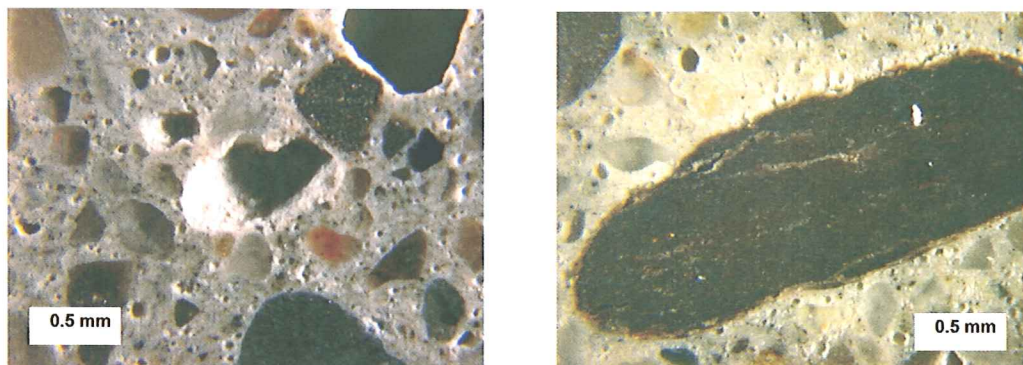


Figure 2. Stereo optical micrograph of typical entrapped air void and cracked siltstone in core A2.

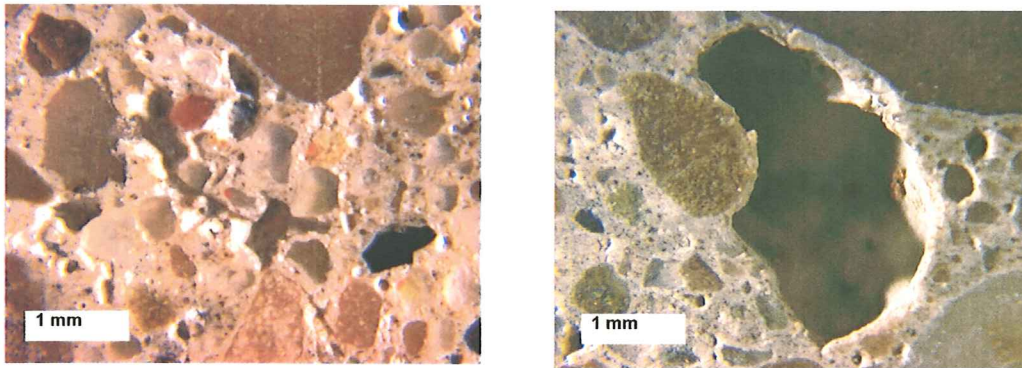


Figure 3. Stereo optical micrographs of entrapped air in specimens B1 (left) and C2 (right).

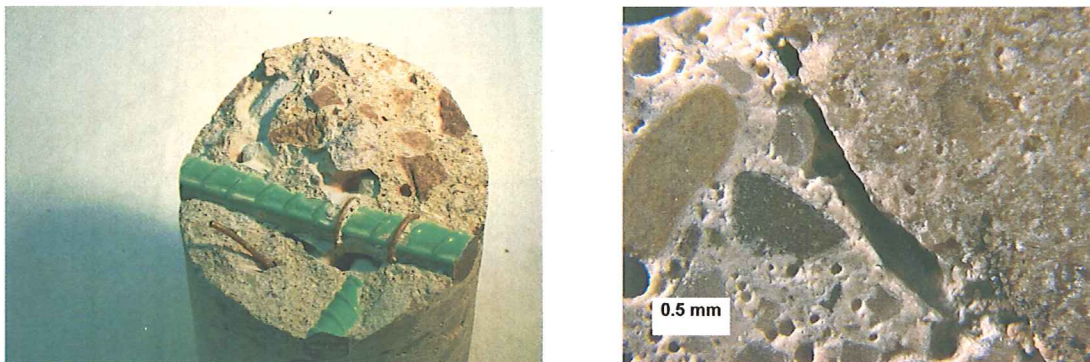


Figure 4. Entrapped air in sample D1, around rebar (left) and aggregate (right).

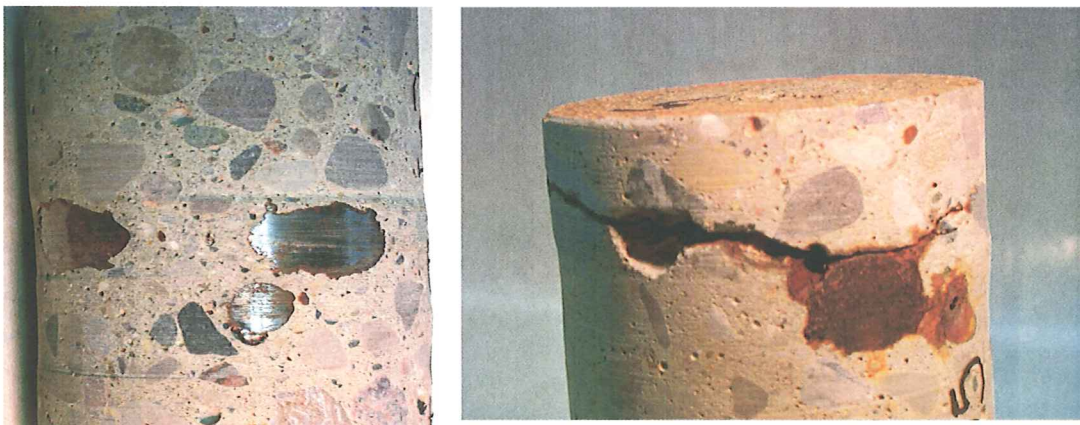


Figure 5. Corrosion of reinforcing steel in cores E1 (left) and E2 (right).

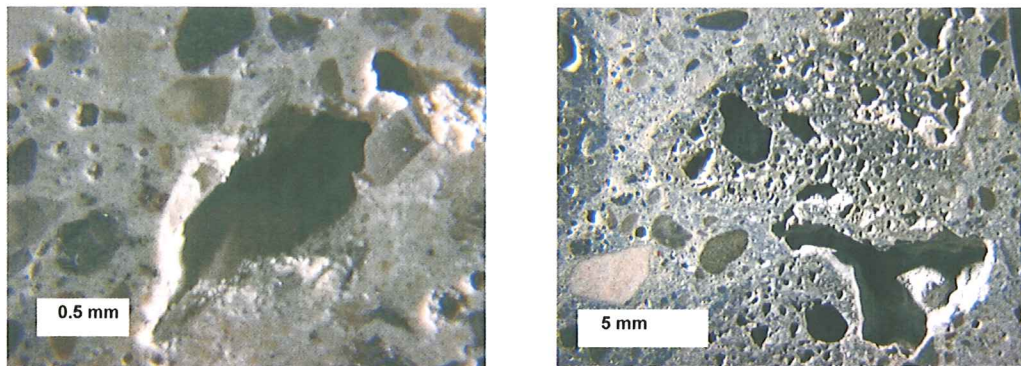


Figure 6. Stereo optical micrographs of entrapped air voids in cores F2 (left) and H1 (right).



Figure 7. Honeycombing in core G2.

As can be seen in table 2 (the highlighting is used to identify samples exceeding recommended limits) and figures 8 and 9, the samples from locations A, B, D, E, all have an adequate spacing factor (< 0.200 mm) and specific surface ($> 25\text{mm}^2/\text{mm}^3$), and no or little filling of the air void system. Samples from location A and B have an air content slightly under the limit normally specified for concrete with 0.75 in maximum size aggregate (6 percent); however, since the other air-void parameters are within safe limits, the protection against freeze-thaw damage should be adequate. For location A, the low air content is due to the very small size of the air voids, while for location B it results from a lower paste content. Figure 10 shows the air-void systems of A2 and D1. Both samples have similar spacing factors, but the air content of A2 is lower because the air-voids are much smaller than in D1.

Table 2. Summary of the air-void system parameters.

| ID MTU | Existing Specific surface (α) mm | Existing Air Content (Area percent) | Existing Spacing Factor (mm) | Paste (Area percent) | Coarse Aggregate (Area percent) | Fine Aggregate (Area percent) | Importance of filled air voids |
|-----------|--|--|---------------------------------------|----------------------------|--|--|-----------------------------------|
| A1 | 40.1 | 5.6 | 0.112 | 26.4 | 37.4 | 30.6 | None |
| A2 | 51.0 | 4.7 | 0.088 | 22.0 | 47.1 | 26.3 | None |
| B1 | 36.1 | 4.2 | 0.123 | 19.0 | 39.1 | 37.7 | Minor |
| B2 | 42.6 | 4.4 | 0.107 | 21.0 | 46.3 | 28.0 | Minor |
| C1 | 35.8 | 6.5 | 0.072 | 16.9 | 50.6 | 25.9 | Minor |
| C2 | 23.7 | 5.0 | 0.206 | 28.2 | 30.3 | 36.3 | Minor |
| D1 | 36.2 | 7.3 | 0.072 | 19.1 | 40.1 | 33.6 | None |
| D2 | 31.0 | 9.3 | 0.076 | 21.9 | 41.0 | 27.8 | None |
| E1 | 28.8 | 7.0 | 0.120 | 24.3 | 42.5 | 26.2 | Minor |
| E2 | 30.4 | 7.7 | 0.096 | 22.5 | 45.7 | 24.2 | Minor |
| F1 | 15.4 | 8.9 | 0.203 | 27.4 | 30.6 | 32.7 | Very Important |
| F2 | 25.4 | 6.6 | 0.173 | 29.2 | 45.6 | 18.4 | Important |
| G1 | 9.9 | 6.0 | 0.434 | 25.1 | 29.8 | 38.0 | Very Important |
| G2 | 3.7 | 7.8 | 0.784 | 22.0 | 39.9 | 29.2 | Very Important |
| H1 | 19.1 | 12.6 | 0.180 | 26.1 | 43.0 | 20.4 | Important |
| H2 | 7.656 | 12.82 | 0.30452 | 28.96 | 28.7 | 28.6 | Very Important |

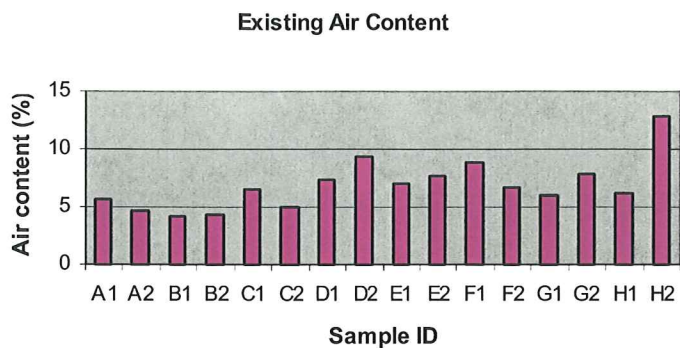


Figure 8. Air content of cores evaluated.

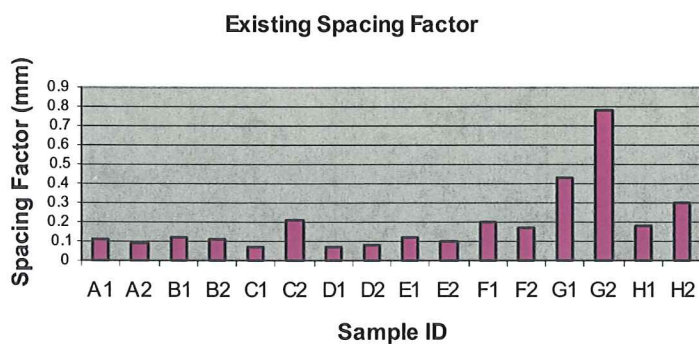


Figure 9. Spacing factor of cores evaluated.

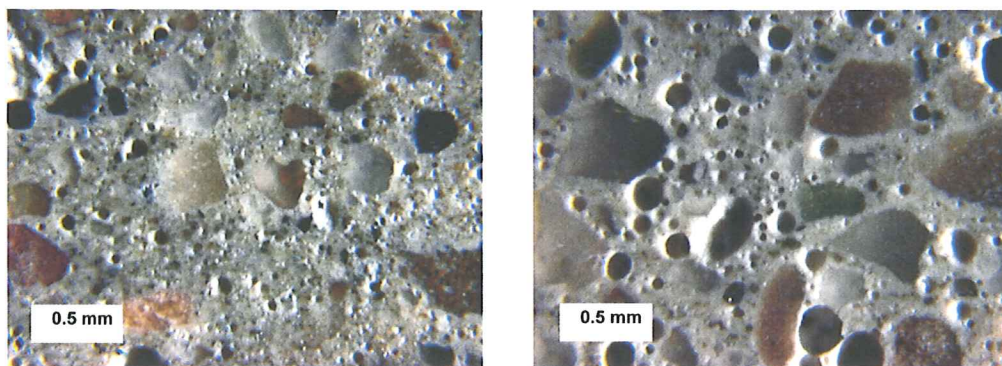


Figure 10. Stereo optical micrograph of air-void structure in A2 (left) and D1 (right).

At locations F and H, the existing air content is well above the specified limit; however, the existing spacing factor is just above or below the limit of 200 μm , depending on the sample. For those two locations, the high spacing factors result from the fact that some air voids are filled with secondary ettringite. Seeing the amount of filled air voids observed, the original air content of these samples was probably grossly over the specified limit and the spacing factor adequate. The two samples from location C show different results, one slab has a spacing factor well below the limit and the other slab has a spacing factor above the limit. Contrary to locations F and H, the high spacing factor in the case of C2 is not due to a large quantity of filled air-voids, but rather to a lack of initial air voids. Figure 11 shows stereo-optical micrographs of the air-void structure in concrete from sites F and C. The white “dots” in concrete from site F are ettringite filled voids.

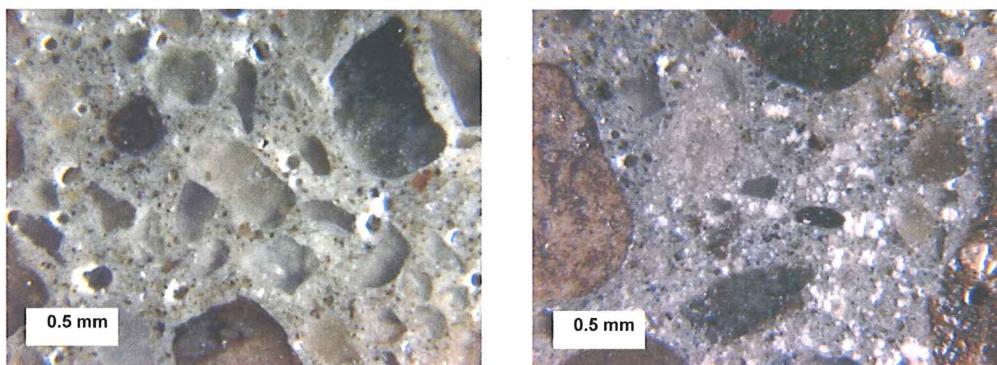


Figure 11. Stereo optical micrographs of air-void structure from C2 (left) and F1 (right).

Samples G1 and G2 are the “worst” with regard to the air-void system. Both samples have high measured air contents only because of the numerous interconnected large entrapped air voids, indicating inadequate consolidation. As can be seen from figure 12, few entrained air voids are present in the concrete and most of them are filled with ettringite (the dissolution and recrystallization of primary ettringite was probably facilitated by poor consolidation), so the existing spacing factor of those slabs is significantly higher than the safe limit, and the barriers are highly susceptible to freeze-thaw deterioration. In these samples, the filled voids were a little easier to distinguish from the paste, so an attempt was made to record the filled air voids during the point count. The original spacing factors (calculated including the filled and empty air voids)

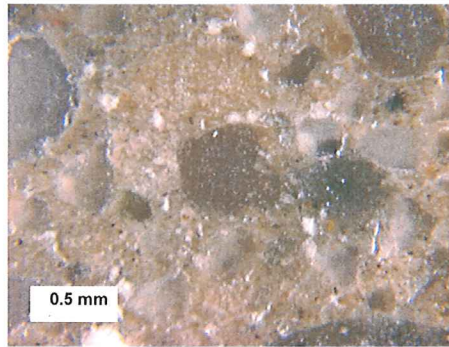


Figure 12. Stereo optical micrograph of air-void system in G2.

were estimated at 0.21 mm and 0.308 mm for G1 and G2, respectively, which are less than half of the existing spacing factors, but still in excess of the 0.2 mm limit. This means that even before the infilling, the amount of air-entrained voids might not have been satisfactory.

4.3 X-Ray Analytical Microscopy

During the inspection with the stereo-optical microscope, signs of alkali-silica reactivity (ASR) were observed in the chert and siltstone fine aggregates of the samples from locations F and H, and some cracked siltstones were noticed in samples from location A. Therefore, several x-ray maps were produced of those samples. Figures 13 and 14 present x-ray maps recorded from samples F2 and H1, respectively. On the left side is the x-ray map presented as an RGB picture, where the red channel is used for the calcium, the green channel for the potassium and the blue channel for the silicon. On the right is a picture of the corresponding location on the sample. Note in figure 13 the high presence of potassium (present in the alkali-silica gel) in the cracks of the fine chert, starting in the aggregate and extending in the paste, and the presence of a cracked black siltstone in the upper right corner.

Figure 14 shows a carbonate aggregate (from H1) containing some inclusions of silicon that seems to be undergoing ASR. Some reacted chert and cracked siltstone can also be observed on the right of the carbonate rock. However, from those maps, and all the other maps that were recorded with the x-ray analytical microscope it is not obvious if the potassium in the siltstones is present as a result of ASR or as a natural constituent of that type of aggregate. This is because it is distributed throughout the aggregates instead of being concentrated in the cracks.

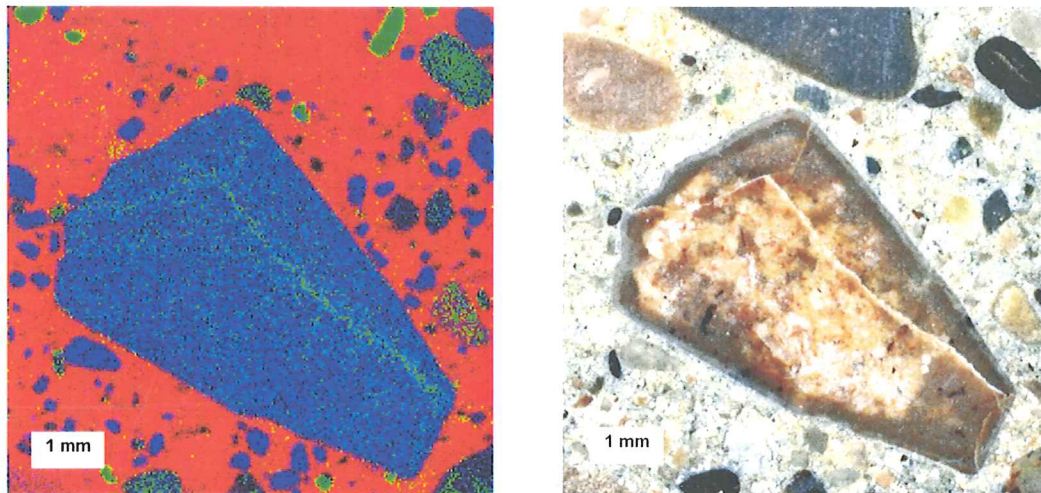


Figure 13. X-ray map (left) and picture (right) of reacted aggregates in specimen F2. Red: Ca, green: K, blue: Si.

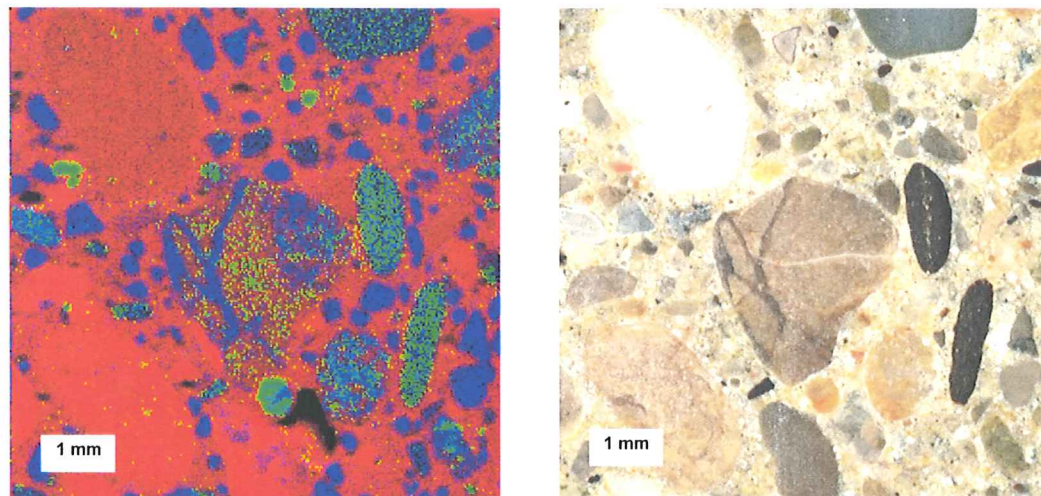


Figure 14. X-ray map (left) and picture (right) of reacted aggregate in core H1. Red: Ca, green: K, blue: Si.

4.4 Petrographic Optical Microscopy

Thin sections confirm the alkali-silica reactivity of the cherts (figure 15), but also of the siltstones in locations F and H (figure 16). Cracks in the fine siltstones from locations F and H clearly extend through the paste, but deposits of alkali-silica gel are more important in location F.

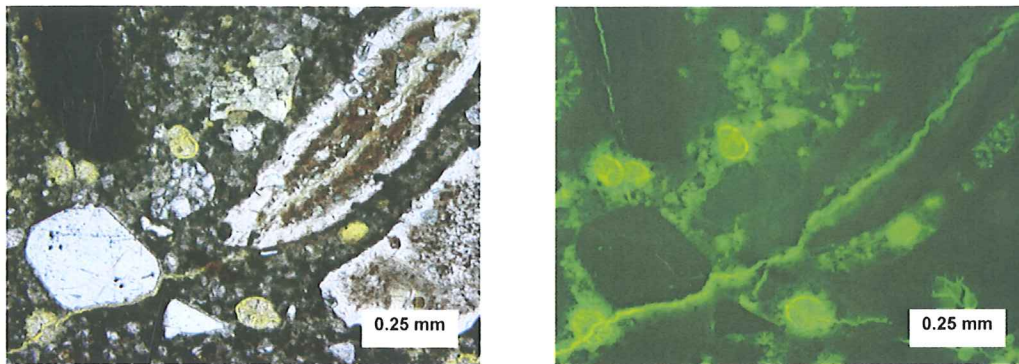


Figure 15. Petrographic micrograph of reacted chert and ettringite filled voids in F1, plane polarized light (left), epifluorescent mode (right).

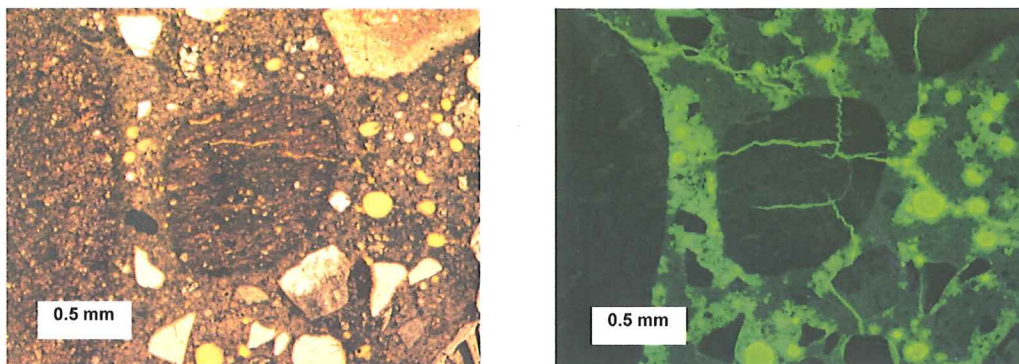


Figure 16. Petrographic micrograph of reacted siltstone in H1, plane polarized light (left), epifluorescent mode (right).

Thin sections from location A, when observed in epifluorescent mode (figure 17), indicate that the cracks in the siltstones do not reach as far from the aggregate, are not as wide open, nor as numerous as for locations F and H. Moreover, no gel was observed in transmitted plane polarized light, so ASR is less probable cause of the cracking unless the reaction is in an early stage. Cracking of the siltstones at location A might be due to freeze-thaw deterioration. Indeed, the siltstone aggregates have a very porous microstructure, and as was also observed in stereo-optical analysis, the boundary between the paste and the fine siltstones was sometimes destroyed, possibly as a result of volume changes or the expulsion of water from the aggregate during freezing and thawing. In the case of locations F and H, the deterioration by ASR linked to the siltstones might also have been aggravated by frost action.

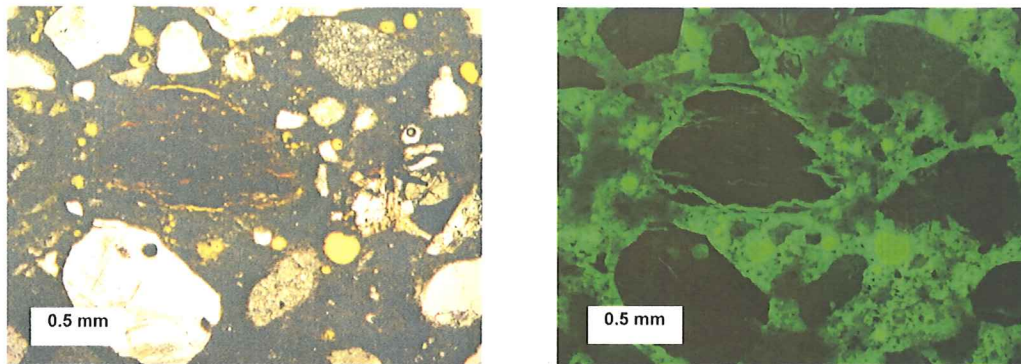


Figure 17. Petrographic micrograph of siltstone in A1, transmitted plane polarized light (left) and epifluorescent mode (right).

Finally, ettringite was observed infilling air voids in thin sections from locations F, G and H. The infilling was particularly important at locations F and G. Figure 18 shows a typical air void filled with needle-like crystals of ettringite from core G2.

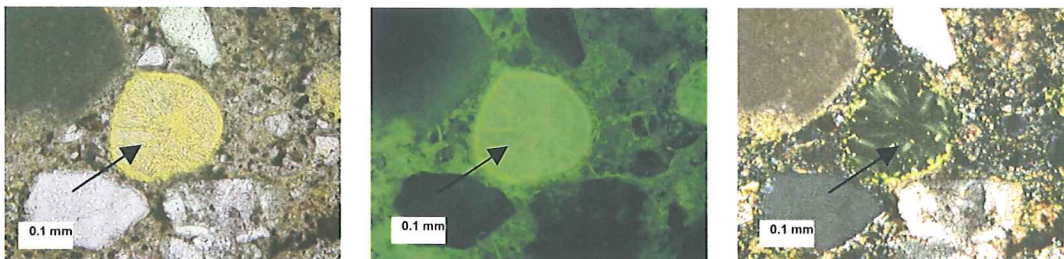


Figure 18. Petrographic micrograph of ettringite filled air void in G2, from left to right plane polarized light, epifluorescent mode and cross polarized light.

4.5 Scanning Electron Microscope Tests

The SEM-EDS was used to supplement the results of the stereo and petrographic optical microscopy. X-ray spectra and x-ray maps confirmed the identity of alkali-silica gel in the cracked siltstones at location F, and of ettringite in air voids from locations F, G and H. No alkali-silica gel was found in the siltstones from location A. Figure 19 shows an SEM image (in backscattered mode) of a cracked siltstone from location F with gel filling the crack and an adjacent air void (indicated with an arrow on the image), and an x-ray spectrum recorded at the location of the infilling, confirming the identity of alkali-silica gel. Figure 20 presents an SEM

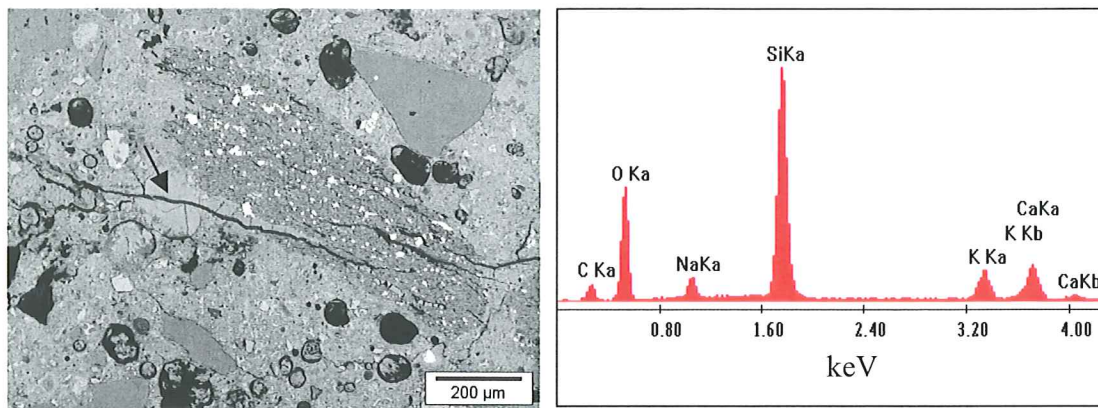


Figure 19. SEM image and x-ray spectra of ASR gel deposit from a reactive siltstone in F1.

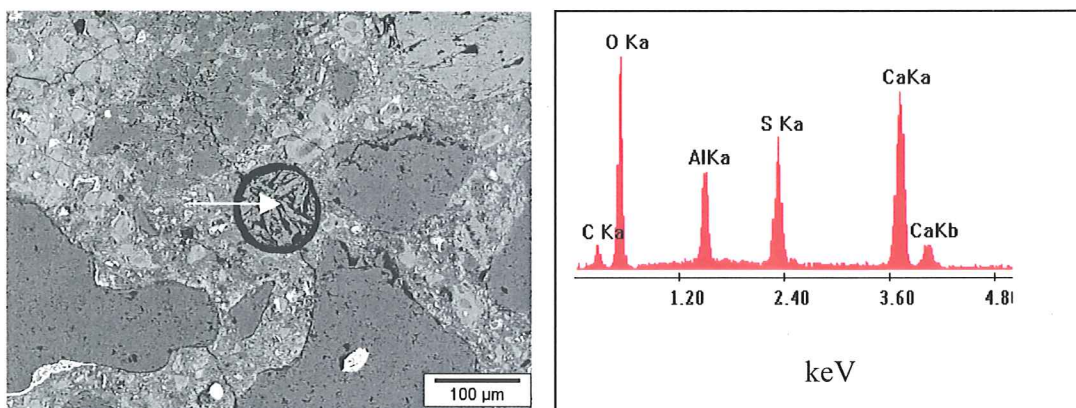


Figure 20. SEM image and x-ray spectra of ettringite infilling air void in G2.

image of a filled air void in G2 with the corresponding x-ray spectrum, confirming the presence of ettringite (calcium sulfoaluminate).

4.6 Carbonation

The depths of carbonation measured from the samples stained with a phenolphthalein solution are summarized in table 3. Where the depth of carbonation was not uniform, which was usually the case, the deepest and shallowest measurements are given.

Table 3. Depth of carbonation.

| Sample ID | Depth of Carbonation (mm) |
|-----------|---------------------------|
| A1 | 1-3 |
| A2 | 1-2 |
| B1 | 2-5 |
| B2 | 2-4 |
| C1 | 2-4 |
| C2 | 1-3 |
| D1 | 1 |
| D2 | 2 |
| E1 | 4-10 |
| E2 | 1.5-4 |
| F1 | 0.5-4 |
| F2 | 1-3 |
| G1 | 2-4 |
| G2 | 1.5-3 |
| H1 | 2 |
| H2 | 1-3 |

In general, the average depth of carbonation was relatively small for all the observed samples, indicating that the outer layer of the concrete does not seem to be abnormally porous. However, samples B, E, and G have an average carbonation depth greater than 2 mm, which might indicate a concrete of lesser quality (density). In samples E and F the depth of carbonation varies greatly, indicating the presence of preferential pathways (e.g. cracks). Part of a phenolphthalein stained polished billet from site F is shown in figure 21, the pink color corresponds to the uncarbonated paste. The great variation of the carbonation depth in concrete F might be related to map cracking present at the surface of the concrete as a result of ASR.

4.7 Summary

Most of the cores examined show at least some consolidation problems; however, size and quantity of entrapped air voids vary greatly among the samples, going from small voids in samples from location A to honeycombing in specimens from location G. The air-void systems of samples A, B, and D are adequate, although the air contents of cores from locations A and B are a little lower than normal. For locations C, F, and H the spacing factor is not adequate.

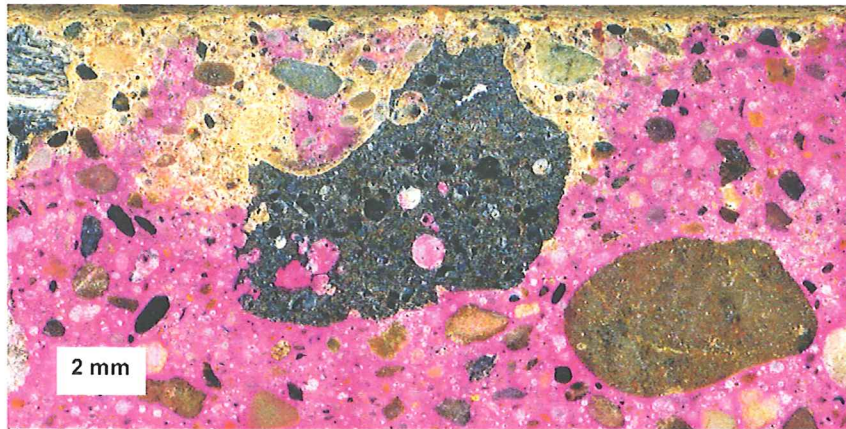


Figure 21. Part of phenolphthalein stained polished slab from F1, showing variation of carbonation along the surface.

In the case of locations F and H, a lot of entrained air voids are present, but most of them are filled, whereas for location C there seem to be a lack of entrained air voids but not much infilling. The cores from location G also have an inadequate spacing factor, due to extensive ettringite infilling of existing air-voids and possibly lack of initial air voids. The barriers at that location are thus susceptible to frost damage.

Evidence of alkali-silica reaction was apparent in several of the fine aggregate particles (cherts and siltstones) of the samples containing slag coarse aggregates (F and H). The reaction is manifest as internal cracking of the fine aggregate particles, often extending out into the surrounding cement paste, and by the presence of alkali-silica gel. The reactive siltstones were also observed to be very porous, and might thus be frost-susceptible in addition to being reactive. The extensive presence of ettringite in the air voids of those samples was probably favored by the increased permeability resulting from the deterioration by ASR.

The siltstones that were observed to be reactive at locations F and H were also observed at location A, but in the case of location A, no gel was present and the cracks did not extend appreciably into the paste. It is thus less probable that the siltstones at location A are undergoing ASR; however, the observed cracks might be a result of freeze-thaw deterioration. The fact that the siltstones at location A are not as cracked in the same manner as in those from locations F and H might be due to the absence of reactive cherts, different environmental conditions,

different mix designs, or simply to the fact that the bridge barriers from location A are relatively young (ASR might be in an early stage), and that the fraction of siltstones in the fine aggregate is smaller than for F and H.

The depth of carbonation of samples from locations B, G and E is a little higher than normal, indicating that these samples might be more permeable to water and aggressive agents (e.g. deicer salts) and more susceptible to corrosion. Corrosion was observed in both samples from location E; in sample E2 it was so severe that it even caused delamination of the concrete at the top of the outermost layer of reinforcing steel.

Chapter 5. Conclusions and Recommendations

In order to identify possible factors contributing to the early deterioration of the current generation of barriers used by MDOT, sixteen cores evaluated from bridge barriers from eight different locations in Michigan. The samples were subjected to a full petrographic evaluation, including stereo and petrographic optical microscopy, x-ray analytical microscopy, and scanning electron microscopy. Based on the results of this investigation, the following conclusions can be drawn:

- All the cores evaluated showed some kind of consolidation problems. Entrapped air voids from varying sizes were common around aggregates and the steel reinforcement. Based on these observations, better consolidation of the concrete barriers is required, as this will minimize the ubiquitous entrapped air that was observed at all locations. This entrapped air reduces the strength of the concrete as well as provides a ready pathways for the ingress of water and aggressive chemical agents (e.g. deicers), reducing the life of the barriers.
- Although no low existing air contents were measured (using ASTM C 457), one third of the samples had air-void spacing factors that are considered marginal for protecting the paste from freeze-thaw damage. These high spacing factors were attributed to a lack of entrained air voids (S12-63172), an extensive amount of infilling (S04-82022, S06-82022), or a combination of the two (S01-44044). It is recommended that the air-void system parameters be verified for the specific job mix formula being used. It is well known that the ability of a given air-entraining agent to create an adequate air-void system is affected by the cement and other admixtures used, and time of mixing. This problem is especially acute in stiff mixtures such as used for slip form paving. Controlling the total volume of air by measure the air content of the fresh concrete is not sufficient to ensure freeze-thaw durability. A more rigorous approach to the assessment of the air-void system parameters of the concrete has the potential to significantly enhance the freeze-thaw durability of these concrete barriers.
- Secondary deposits of ettringite were observed in the air voids of several of the cores evaluated in this study. It would be useful to determine the sulfate content of the samples to

evaluate if there is any relationship between sulfate content and amount of infilling. The determination of the sulfate content would be particularly interesting in the case of the concrete with slag coarse aggregate, because based on previous research conducted at Michigan Tech, the dissolution of calcium sulfide from blast furnace slag aggregates may provide an internal source of sulfate possibly promoting the formation of secondary ettringite (Peterson 1999, Hammerling 1999, Hammerling 2000).

- Alkali-silica reactivity (ASR) was observed in the natural fine aggregate fraction at the two locations where blast furnace slag coarse aggregate was used (S04-82022 and S06-82022). It is recommended that a study be initiated to evaluate the nature of the relationship between ASR in the chert and siltstones constituents of the fine aggregates and the slag coarse aggregate in the concrete. This study would need to consider a broad range of factors including the alkali content of the cement, the impact of supplementary cementitious materials, and the type and volume of reactive constituents in the fine aggregate.
- Siltstones observed in concrete from site S041-63174 were similar to those undergoing ASR, but were not reactive. But limited damage was observed that is attributable to freeze-thaw deterioration. The frost-susceptibility of the siltstones, as well as the presence of secondary ettringite in air voids, might also have exacerbated the distress caused by ASR in locations S04-82022 and S06-82022. Tests should be conducted to evaluate the frost-susceptibility of the deteriorated fine siltstones observed at some locations to determine its contribution, if any, to the observed deterioration.
- Finally, significant steel corrosion was observed for only one test site (S02-23152). In that case the corrosion was so severe that delamination had occurred. The carbonation depth measured in samples obtained from this location were higher than normal, indicating that the corrosion might result from a higher permeability to water and aggressive agents (e.g. deicers). Abnormally high permeability could be the result of poor consolidation or the use of a high water-to-cement ratio mixture.

Chapter 6. References

- ACI (1998), *State-of-the-Art report on Alkali-Aggregate Reactivity*, ACI 221.1R-98, 31p.
- ASTM C 457-90*, Standard Test Method for Microscopical Determination of Parameters of the Air-Void System in Hardened Concrete.
- Collins, J. and P. D. Bareham (1986), "Alkali-Silica Reaction: Suppression of Expansion Using Porous Aggregate", *Cement and Concrete Research*, vol. 17, Pergamon Journals, LTD., pp. 89-96.
- Detwiler, R. J., and L. J. Powers-Couche (1999), "Effect of sulfates in concrete on their resistance to freezing and thawing", *Ettringite the Sometimes Host of Destruction*, Farmington Hills, MI, ACI SP 177-12, Bernard Erlin, pp.219-247.
- DePuy, G.W. (1994), "Chemical Resistance of Concrete", *Significance of Tests and Properties of Concrete and Concrete Making Materials*, American Society for Testing and Materials, STP 196C, Philadelphia, PA. pp. 263-281.
- Dobie, T.R. (1986), "Correlation Water-soluble alkalies to Total Alkalies in Cement-Considerations for Preventing Alkali-silica Popouts on Slabs", *Alkalies in Concrete*, ASTM STP 930, V.H. Dodson, ED., American society for testing and materials, pp. 46-57.
- Fagerlund, G. (1997), "On the service life of concrete exposed to frost action", *Freeze-Thaw durability of Concrete*, E&FN Spon. ISBN: 0-419-20000-2, pp. 23-39.
- Famy, C., and H.F.W. Taylor (2001), "Ettringite in Hydration of Portland cement Concrete and its Occurrence in Mature Concretes", *ACI Materials Journal*, vol. 98, no. 4, pp. 350-356.

FHWA (1997), *Petrographic Methods of Examining Hardened Concrete: a Petrographic Manual*, US Department of Transportation, Federal Highway Administration, FHWA-RD 97-146.

Fournier, B., M. Berubé, and C.A. Rogers (1999), "Proposed Guidelines for the Prevention of Alkali-Silica Reaction in New Concrete Structures", *Transportation Research Record 1668: Concrete in Pavements and Structures*, Transportation Research Board, Washington, D.C, pp. 48-59.

Goldstein, J., D. Newbury, D. Joy, C. Lyman, P. Echlin, E. Lifshin, L. Sawyer, and J. Michael (2003), *Scanning Electron Microscopy and X-ray Microanalysis*, Kluwer Academic/ Plenum publishers, New York, p. 689.

Guédon, J.S., and A. Le Roux (1994), "Influence of Microcracking on the Onset and Development of the Alkali Silica Reaction", *Durability of concrete*, Third International Conference, Nice, France, ACI SP-145, V.M. Malhotra, pp. 713-720.

Hammerling, D.M. (1999), "Calcium sulfide in Blast Furnace Slag used as Concrete Aggregate", Thesis for the Degree of M.S., Michigan Technological University, p. 70.

Hammerling, D.M., K.W. Peterson, L.L.Sutter, T. J. Van Dam, and G. R. Dewey (2000), "Ettringite: not just in Concrete", *Proceedings of the 22nd International Conference on Cement Microscopy*, Montreal, Canada.

Hazrati, K., C. Abesque, and M.Pigeon (1997), "Efficiency of Sealers on the Scaling Resistance of Concrete in Presence of Deicing Salts", *Freeze-Thaw durability of Concrete*, E&FN Spon., pp.165-196.

Helmuth, R., and D. Stark (1992), "Alkali-Silica Reactivity Mechanisms", The American ceramic society, Westerville, OH. ISBN 0-944904-55-6, pp. 131-208.

Ho, D.W.S, and R. K. Lewis (1987), "Carbonation of Concrete and its Prediction", *Cement and concrete research*, Vol 17, pp. 489-504.

Hunt, D.M., and L. A. Tomes (1962), "Reaction of Hardened Portland Cement Paste with Carbon Dioxide", *Journal of Research of the National Bureau of Standards-A, Physics and Chemistry*, Vol. 66A, no 6, pp. 473-481.

Jacobsen, S, and E.J. Sellevold (1997), "Frost/salt Scaling and Ice Formation of Concrete: Effect of Curing Temperature and Silica Fume on Normal and High Strength Concrete", *Freeze-Thaw durability of Concrete*, E&FN Spon. ISBN: 0-419-20000-2, pp. 93-105.

Johansen, V, N. J. Thaulow, and J. Skalny(1993), "Simultaneous Presence of Alkali-Silica Gel and Ettringite in Concrete", *Advances in Cement Research*, vol. 5, no17. pp. 23-29.

Johnston, C.D. (1994), "W/cm Code Requirements Inappropriate for Resistance to Deicer Salt Scaling, *Durability of concrete*. Third International Conference, Nice, France, ACI SP-145, V.M. Malhotra, pp. 85-93.

Krogh, H. (1975), "Reaction of Silica and Alkalies", Symposium on Alkali-Aggregate Reaction Preventive Measures, Reykjavik, august 1975, pp. 132-159.

Lane, D.S. (1992), "Alkali-Silica Reactivity: An Overview of a Concrete Durability Problem", *Materials, Performance and Prevention of Deficiencies and Failures*, Proceedings of the Materials Engineering Congress, Atlanta, GA., American Society of Civil Engineers, New York, pp. 231-244.

Litvan, G.G. (1978), "Freeze-thaw durability of porous materials", *Durability of building materials and components: proceedings of the first international conference*, ASTM special technical publications 691, pp. 455-463.

Marchand, J., E.J. Sellevold, and M.Pigeon (1994), “The deicer salt scaling deterioration of concrete – An overview”, *Concrete Durability*, Third International Conference, Nice, France, ACI SP-145, V.M. Malhotra, pp. 1-25.

Mindess, J., F. Young, and D. Darwin (2003), *Concrete*, Prentice Hall, Pearson Education, Inc., Upper Saddle River, NJ 07458, 644p.

Ouyang, C and O. J. Lane (1999), “ Effect of Infilling Air Voids by Ettringite on Resistance of Concretes to Freezing and Thawing”, *Ettringite the Sometimes Host of Destruction*, Farmington Hills, MI, ACI SP 177-12, Bernard Erlin, pp. 249-261.

Petereson K.W., D. Hammerling, L.L. Sutter, T. J. Van Dam, and G.R. Dewey (1999), “Oldhamite: not just in Meteorites”, *Proceedings of the 21st International Conference on Cement Microscopy*, Las Vegas, NV, April 25-29.

Peterson, K. (2001), *Air void analysis of hardened concrete via flatbed scanner*, Thesis for the degree of Master of Science, Michigan Technological University, 39p.

Pigeon, M., and R. Plateau (1995), “Durability of Concrete in Cold Climates”, E&FN Spon, 244p.

Pleau, R. (1992), *La caractérisation du réseau de bulles d’air dans le béton durci comme outil d’évaluation de la durabilité au gel du béton*, PhD Thesis, Laval University, Québec.

Poole, A.B., and A. Thomas (1974), “A Staining Technique for the Identification of Sulphates in Aggregates and Concrete”, *Mineralogical magazine*, September 1975, vol. 40, pp. 315-16.

Rösli, A., and A.B. Harnik (1980), “Improving the Durability of Concrete to Freezing and Deicing Salts”, *Durability of Building Materials and Components*, ASTM STP 691, P.J. Serada and G.G. Litvan , EDS. , American Society for testing and Materials, pp. 464-473.

Scrivener, K.L. (1996), "Delayed ettringite formation and concrete railroad ties", *Proceedings of the 18th International Conference on Cement Microscopy*.

Shoya, M. (1997), "Freezing and Thawing Resistance of Concrete with Excessive Bleeding and its Improvement", *Durability of concrete*, Proceedings Fourth CANMET/ACI International Conference, Sydney, Australia, Volume 2, ACI SP-170, V.M. Malhotra, pp. 879-887.

Staton, J.F. and Knauff, J. (1999), "Performance Evaluation of Michigan's Concrete Barriers," Draft Report, Materials Research Group, Construction and Technology Division, Michigan Department of Transportation, Lansing, MI. January.

Stark, J., and K. Bollmann (1999), "Laboratory and Field Examination of Ettringite Formation in Pavement Concrete", *Ettringite the Sometimes Host of Destruction*, Farmington Hills, MI, ACI SP 177-12, Bernard Erlin, pp. 183-191.

Stark, J., and J.M. Ludwig (1997), "Influence of Water Quality on the Frost Resistance of Concrete", *Freeze-Thaw durability of Concrete*, E&FN Spon, pp.157-164.

St John, D. A., A W. Poole, and I. Sims (1998), *Concrete Petrography, a Handbook of Investigative Techniques*, Arnold, 474p.

Sutter, L. L. (2001), *An approach to Characterize Materials Related Distress in Portland Cement Concrete Pavements*, Dissertation for the Degree of Ph. D., Michigan Technological University, 294p.

Van Dam, T. J., L.L. Sutter, K.D. Smith, M.J. Wade, and K.R. Peterson (2002a), *Guidelines for the Detection, Analysis, and Treatment of Materials-Related Distress in Concrete Pavements - Volume 1: Final Report, FHWA-RD-01-164*, Federal Highway Administration, McLean, VA.

Van Dam, T. J., L.L. Sutter, K.D. Smith, M.J. Wade, and K.R. Peterson (2002b), *Guidelines for the Detection, Analysis, and Treatment of Materials-Related Distress in Concrete Pavements -*

Volume 2: Laboratory testing, Data Analysis, and Interpretation Procedure for Distressed Concrete Pavements, FHWA-RD-01-164, Federal Highway Administration, McLean, VA.

Ymashita, H., K. Sakai, and T. Kita (1997). "Effect of Pore Structure in Concrete on Frost Resistance", *Durability of Concrete*, Proceedings Fourth CANMET/ACI International Conference, Sydney, Australia, Volume 2, ACI SP-170, V.M. Malhotra, pp. 919-925.